Preprints of the 21st IFAC World Congress (Virtual)
Berlin, Germany, July 12-17, 2020

Reference Trajectory Generation for Closed-Loop Control of Electrical Stimulation for Rehabilitation of Upper Limb

Tarun Karak*,[1]. Laxmi Kant Tiwari*,[2]. Somnath Sengupta*,[3]. Sudip Nag,[4]**

**Advanced Technology Development Centre, IIT Khargpur, Kharagpur, India ** Electrical & Electronics Communication Engineering Department, IIT Khargpur, Kharagpur, India*
email: [1]tarunkarak@iitkgp.ac.in, [2]laxmimerit@gmail.com, [3]somnath.el21@gmail.com, [4]sudipnag1@ece.iitkgp.ac.in

Abstract: Functional movements in the paralyzed upper limb can be restored with the help of brain-computer-interface (BCI). A BCI system typically adopts a functional electrical stimulation (FES) system that activates weakened muscles that are otherwise responsible for actuating finger movements. A BCI-FES system can enable muscle contraction through the delivery of electrical stimulation pulses. The control of voltage or current stimulation parameters such as pulse width, frequency, and amplitude along with feedback signals from finger joints positions are essential for stable grasping. For the design of a closed-loop functional electrical stimulation controller, it is obligatory to set standard reference trajectories of finger joints' angular positions and velocities for controlling stimulation parameters in neuroprosthetics and rehabilitation. This study proposes a new closed-loop control architecture targeted for achieving successful and stable grasping of an upper limb paralyzed subject. This can be achieved by characterizing each of the finger joints' instantaneous angular position and velocity, through reference trajectories. These reference trajectories are generated corresponding to various types of grasping for feeding to the controller, responsible for stimulation of muscles. Hence, to generate such trajectories, first, grasping classification has been implemented using standard machine learning algorithms on a large set of existing real-time data of different types of objects' grasping such as various diameter, abducted thumb and other types of objects, from many healthy subjects. The results demonstrate the successful implementation of fairly accurate classifications and trajectory generations which are crucial for closed-loop control towards stable grasping.

Keywords: BCI, FES, EMG, EEG, closed-loop control, trajectory generation, classification of grasping, machine learning.

1. INTRODUCTION

Worldwide, millions of people experience *spinal cord injury* (SCI), stroke and other nerve diseases which lead to loss of voluntary limb movements, as the signal pathway between the brain and the muscles are disrupted (Chad et al., 2018). Currently, over 90 million people worldwide suffer from SCI and become paralyzed while spending an average of 40 years in wheelchairs (Zhan et al., 2018). For the *activity of daily life* (ADL), our hand plays an essential role in grasping different objects. Therefore, the restoration of functional movement would provide the most significant practical benefit for an upper limb paralyzed person. *Functional Electrical Stimulation* (FES) can be used as a *neural bypass system* (NBS) to restore the motor function by delivering electrical pulses to paralyzed or weakened muscles using surface electrodes on the forearm. Several forms of closed-loop methods have been proposed for FES that have induced better adaptability and smaller steady-state error (Zhan et al., 2018). Recently, the cortically recorded signal has been used to trigger an FES system and deliver electrical pulse on the forearm by surface electrodes for the restoration of functional movements (Chad et al. 2018) and the same enables graded control of muscles' contraction (Friedenberg et al., 2016). A feature-based classification model of *electroencephalography* (EEG) signals has been developed to decode the grasp pattern from the motor imagery signal and estimate the fingertip force (Roy et al., 2016, Mattar et al., 2017, Sburlea et al., 2018). Two broad categories of grasp pattern, power grasp and precision grasp were classified in the alpha sub-band (Roy et al., 2016). Recently, *model predictive control* (MPC) has been used for smooth grasp and release tasks and to control stimulation parameters on the muscles (Westerveld et al., 2012). The obtained MPC results have been compared with a Proportional (P) controller for the same application, and it was found that MPC takes less time for tracking the reference trajectories. However, all the mentioned systems have not been able to achieve stable grasping for all types of objects, and they lack selectivity, comfort, accuracy and the convenience of using the respective technology in rehabilitation.

The broad aim of this work is to develop strategies and reference trajectories that may be used in a closed-loop control system for assisting a stable and smooth grasping, only applicable for people with forearm muscles who can perform sufficient grasping by themselves for different types of objects, thereby restoring voluntary control of paralyzed

patients. The set of suitable criteria for the reference trajectories thus generated are achieved by studying, interpreting and characterizing the angular positions and velocities of every finger joints for different types of object during their successful grasping. To fulfil the real-life daily needs of standard 33 types of grasps that are reported in literature Feix et al. (2009), a large set of an existing dataset that has been collected by '*CyberGlove'* has been used to classify them using standard machine learning algorithms. Based on the classified grasping, the set of characterizing (finger joints) angular position and velocity trajectories have been generated corresponding to each grasping using suitable curve fitting techniques to ensure smooth grasping.

2. PROPOSED SYSTEM DESCRIPTION

The closed-loop control architecture proposed for this work to achieve stable grasping of paralyzed patients adopts an EEG based data acquisition as it can measure cortical activity with a temporal resolution of less than a millisecond (Roy et al. 2016). The overall system architecture has been depicted in Fig.1. The acquired motor imagery signals from EEG will be classified according to the intended grasping of a particular object (Esmeralda et al., 2016, Mattar et al. 2018), so as to discriminate the various movements with an upper limb (Yong et al. 2015). The classified grasping type will enquire corresponding kinematic data of each finger joints' movement from the database as indicated in the first block inside the dotted block. From these kinematic data of finger joints, reference trajectories will be generated for angular positions and velocities. These reference trajectories will be used by respective position and velocity controllers to calculate the error from the actual finger motion. These errors will be used by final controller to control stimulation parameters. The final controller compute stimulation parameters by taking muscles excitation response through EMG along with kinematic errors. For a stable and smooth grasping, an FES system will inject current stimulation on corresponding muscles for assisting to grasp in closed-loop operation.

To achieve these functionalities, a large set of existing kinematic data of angular joint positions have been used to classify the grasping types using machine learning algorithms as shown in the first block, inside the dotted box. The kinematic data has been used to classify grasping type due to non-availability of EEG data, currently. This existing data set of 33 types of objects' grasping have been further used to find the reference trajectories of 16 joints' instantaneous angular positions and their velocities with a confidence bound of 95%. Based on this confidence bound, it creates an envelope of upper and lower bounds around the generated trajectory (angular positions and velocities for different grasping). Now, these reference trajectories for angular positions and velocities of each of the finger joints, along with its upper and lower set-point values (corresponding to upper and lower bounds), are fed to the respective position and velocity controller. Further, based on the error w.r.t. feedback from actual angular positions and velocities, the respective position and velocity controllers generate corrective control inputs that are fed to the final controller, which are responsible for computing the stimulation parameters for the FES system. The final controller, as shown in Fig.1, will help to decide to set the voltage or current stimulation parameters such as pulse width, frequencies and amplitudes. A multichannel programmable FES system will typically generate the stimulation by surface electrodes placed on the forearm's muscles such as *Flexor Digitorum Profound* (FDP), *Flexor Digitorum Superfilcialis* (FDS), *Palmaris Longus* (PL) and *Extensor Digitorium* (ED), *Adductor Policis* (AP), *Palmar Interossei* (PI), *Abductor Policis Longous* (APL), *Abductor Digitorum Minimi* (ADM)

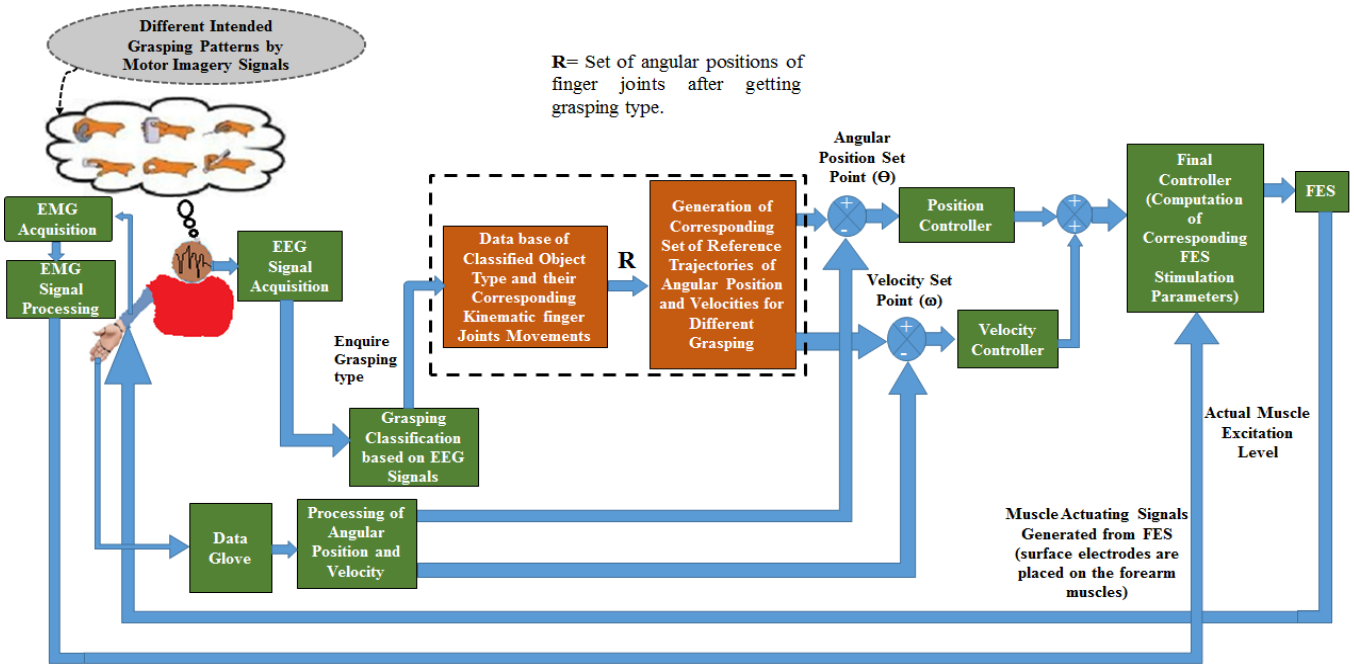

Fig.1: Proposed the architecture of a closed-loop (EEG and EMG based) bionic grasping system.

and *Dorsal Interssei* (DI) for actuating corresponding tendons. Due to the activation of these muscles, finger joints such as *Carpometacarpal* (CMC, only for thumb), *Metacarpophalangeal* (MCP), *Proximal Interphalangeal* (PIP) and *Dorsal Interphalangeal* (DIP) of each finger will displace and help to grasp an object (Bandara et al., 2014). The stimulation on the corresponding flexion and extension muscles simultaneously will actuate and will help to move each finger joints for grasping a particular object. Initially, we will consider a data-driven model for muscle dynamics and actuation by FES while grasping an object. In future, we will develop a mathematical or state-space model for extrinsic and intrinsic muscles for more accurate analysis, as described in Freeman.C (2015).

The angular position and velocity acquired from the *'Data Glove',* worn by the subject, can be further processed. As mentioned in the controller actuation part, the angular positions and velocities are given as feedback to the respective controller for error correction. An EMG acquisition system is further used to record the muscles' excitation levels. These EMG signals, along with the motion data, have been used as feedback to the controller and can re-compute the desired stimulations parameters. The system can thus operate in a closed-loop manner for stabilized and smooth grasping. Based on the muscle model and its response, we will develop and fine-tune the control strategies before actually implementing for a real subject. This work mainly considers healthy subjects with no plasticity in their muscles, while, for SCI patients, we will consider subjects having partial or less muscles spasticity. The theoretical basis of the grasping classifications and trajectories generation block are explained in the subsequent section.

3. GENERATION OF TRAJECTORIES THROUGH GRASPING CLASSIFICATION

The objective of the proposed work is the restoration of voluntary movement in upper limb paralyzed patients by using a closed-loop control system and strategy as proposed in Fig.1. This section focuses on the generation of the trajectories (highlighted or the dotted block) which follows the grasping classifications step for the intended grasp, which is inferred from EEG. These generated dynamic trajectories of position and speed serve as reference profiles having upper and lower bounds for the purpose of generation of appropriate stimulation parameters by the final controller for actuating the FES and ensure stable grasping.

3.1 Classification of Grasping:

Humans have the ability to grasp different objects having various shapes, sizes and dimensions. This includes objects that are cylindrical, spherical, pen, disk, card and other shapes and have large/small dimensions or diameters. Feix et al. (2009) incorporated 33 types of different standard tasks, and the same has been considered for this work. Thirty healthy right-handed subjects (15 males and 15 females, the average age of 25 years) participated with written consent (Feix et al., 2009). The 'CyberGlove' embedded 16 sensors placed on each finger joints (j = 1…16) that are namely MCP, PIP, DIP for four fingers (index (I), middle (M), ring (R) and little (L)), as well as CMC, MCP, inter-phalangeal IP, abduction ABD for the thumb. Samples of time-stamped angular positions (in Degrees) were collected during each grasping activity. As depicted in the system description, when an upper limb paralyzed person intends to grasp an object, it is essential to know the type of object, so that each finger will move accordingly to make a stable grasp. From the referenced data (Feix et al., 2009), a scheme for implementing the generation of a supervised predictive classification model of grasping types along with their validation has been illustrated in Fig.2. The raw data taken for implementing the classified predictive model is represented by the "Raw Data" block of Fig.2. As 30 subjects had participated in the experiment, duration of grasping time for each individual subject is found to be different for grasping the same type of object. In order to get a normalized time for all subjects, the raw data was pre-processed (shown by "Data pre-processing" block in the figure) by using an interpolation method. The instantaneous angular positions of each finger joints varying with time have been chosen as features for *principal component analysis* (PCA). The main goal of the PCA algorithm is extracting meaningful information by re-expressing noisy data (Paul et al., 2013). All the values of input variables chosen for feature extraction are centered by subtracting the mean from each input variables (Paul et al., 2013). Therefore, it can be ensured that the resulting components (during PCA) will use the variances within the dataset rather than capturing the overall mean of the dataset as essential variables. By using this centered data set or adjusted data set (denoted as A), a covariance matrix is formed to get the largest eigenvalues and eigenvectors. From the eigenvalues and eigenvectors, the purpose of reducing dimensionality is achieved, while, the eigenvector that forms the highest eigenvalues is considered to be the principal component (Paul et al., 2013).

A successful and stable grasp of any object requires the combined and simultaneous actions of at least two or three fingers, such as thumb, index and middle (Santello et al., 2002) in a well-coordinated manner. Among the 16 finger joints belonging to the 5 fingers, 10 finger joints are considered for correlation with each other for characterizing the grasp, because of their high variances. These joints are CMC, ABD, MCP and IP of thumb (finger joints number = 1,2,3,4), MCP, PIP and DIP (finger joints number = 5,6,7,8,9,10) of both finger index and middle and have been chosen for PCA. So, to get the final data set, we have chosen 10 principal components out of 16 angular position values during grasping of a particular object. Therefore, the feature vector can be formed as in (1) Paul et al. (2013).
The final data set has been generated with the extracted feature vector (Paul et al., 2013) and expressed in (2).

$$Feature\ Vector = X = [x_1, x_2, \ldots, x_{10}] \quad (1)$$

Final Data Set = Row Feature Vector × Adjusted Data

$$X^T \times A^T = C \quad (2)$$

Where, Row Feature Vector matrix has been formed by transposing the columns of the eigenvectors so that the most significant eigenvector is on the top, and the centred data set

(*A*) is transposed to get the adjusted data set. The final data set (*C*) has been distributed between predictive model training (80 %) and testing (20 %) as shown in the Fig.2. The model has been trained with 80 % data set along with the 33 types of grasping or labels such as large diameter, small diameter along with others, for generating the predictive classification model. The generated predictive model with the highest accuracy can be used for further validation. When a new subject will intend to grasp an object, shown in the subsequent block (new subjects grasping), a corresponding new set of angular joints' position will be generated. The raw data comprising the angular positions can be pre-processed for feature extraction, as explained earlier in the generation of the predictive model. These features extracted vectored data can further be used as inputs to the generated predictive classification model to get the corresponding grasping type as intended by the subject.

3.2 Generation of reference trajectories of angular positions and velocities

The final angular positions of each finger joint play the most important role for the intended smooth and stable grasping. Based on the classified grasping type, explained as per Fig. 2, the proposed system generates the reference trajectories of angular positions and their velocities for each joint from the initiation of grasp to the final successful contact of the object being grasped. These trajectories of angular positions from beginning till the last angular position will help the controller

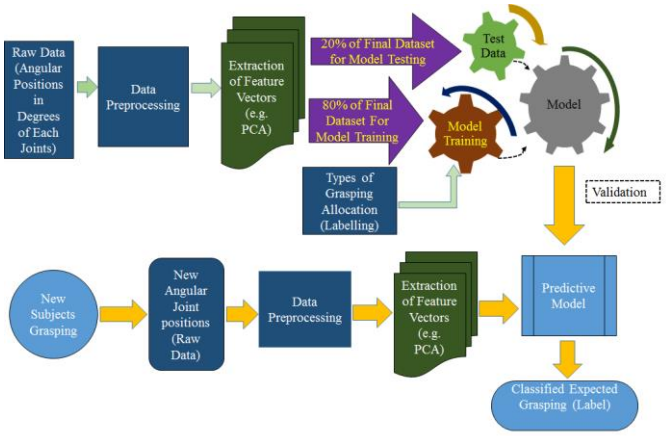

Fig.2: Predictive classification model generation and validation.

to decide the stimulation parameters. During the grasping, the velocities of each finger joints are also important to be characterized, since, as the velocities increase or decrease they will affect the stability of the grasping. So, the angular velocities have been calculated as in (3).

$$\omega_n(t) = \frac{\theta_n(t) - \theta_{n-1}(t)}{t_n - t_{n-1}} \tag{3}$$

Where, $\omega_n(t)$, $\theta_n(t)$ and t_n are the present angular velocity, position and time instant. A set of successive iterations of velocities, $\omega_1(t)$, $\omega_2(t)$,… $\omega_n(t)$, along the entire grasping duration will generate a continuous reference path for each finger joints. This continuous path can be used as a reference velocity trajectory to achieve the final stable angular position for smooth or natural grasping. The criteria for generating the trajectories is the correlation of each finger joints as well as average value of the minimum and maximum angular positions of all the finger joints for each type of grasping, being considered.

The trajectories are generated using curve fitting techniques with different functions such as polynomials (up to 8th), sum of sines, smoothing spline functions and others which result in conceiving performance metrics such as the sum of square error (SSE), root mean square error (RMSE), R-square value and adjusted R-square value. Fig.3 (a) and (c) show the typical nature of trajectories of angular position and velocities along with their envelopes of lower and upper bounds of the Carpometacarpal joint of the thumb (T_CMC). The corresponding residual (the difference between response value and the predictor value) plots shown in Fig. 3 (b) and 3(d) during grasping a large diameter object. This trajectory is to be followed by the finger joints for stable grasping. The trajectory for the angular position and velocity with time can be generated up to nth order (can go up to 8) polynomials. Fig.3 (a) shows a typical trajectory for the angular position with a time of 4th order polynomial expressed in equation (4) of thumb's CMC joint.

$$\theta(t) = \sum_{i=1}^{N=5} P_i * t^{N-i} \tag{4}$$

Where (N-1=n) represents the order of the polynomial and P_i is the constant coefficient. In the trajectory plot, this polynomial is fitted with the value of actual mean angular position with time and generates performance metrics such as SSE, RMSE, R-square and adjusted R-square. When, the values SSE and RMSE are closer to 0 indicates that the model has smaller random error, further signifying that the predicted model will be more accurate. If the values of R-square and adjusted R-square are close to 1, they are considered to be the best fitted curve. The residual's data point closer to zero lines signifies better curve fitting. It is to be noted that the trajectories have been generated by considering zero initial velocity and the time. Fig.3(c) shows the trajectory generation of velocity with time of 4th order for thumb's CMC and the corresponding polynomial is represented by equation (5) and Fig.3 (d) shows the corresponding residual plot.

$$\omega(t) = \sum_{k=1}^{N=5} B_i * t^{N-k} \tag{5}$$

Where, (N-1 = n) is the order of the polynomial and B_i represent the constant coefficient of polynomial. The generated trajectories have the confidence bound of 95% with upper and lower bound. The generated trajectory should be within the envelope created by lower and upper bound so that it can reach to the final grasping angular position in a more stable way. A set of generated trajectories (instantaneous angular position and velocity) is made for 33 types of grasping averaged over 30 subjects and for each of their corresponding 16 finger joints. To characterize the trajectory of the angular position and velocity simultaneously with time, a typical 3D plot is shown in Fig. 4.

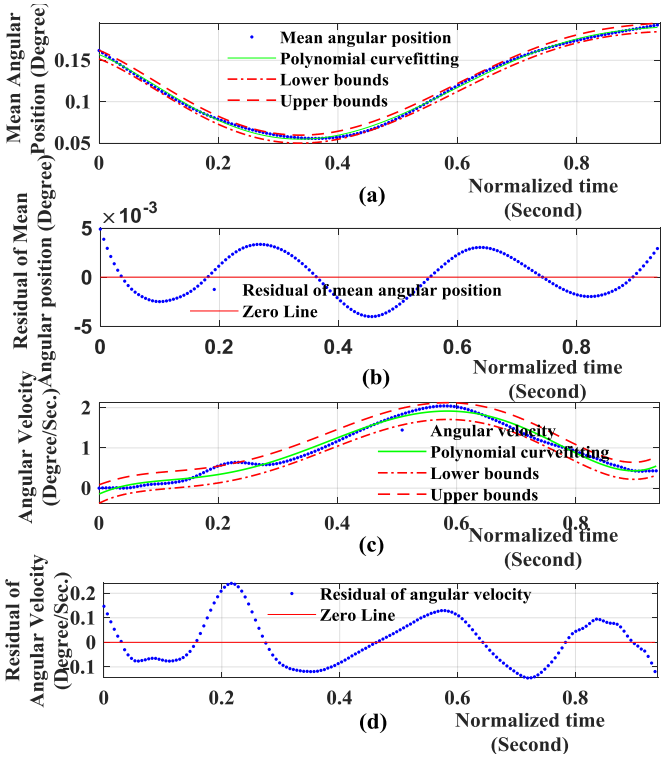

Fig. 3: Trajectory of (a) Angular position plot and (c) velocity with time of thumb's CMC, (b) and (d) are corresponding residual plots.

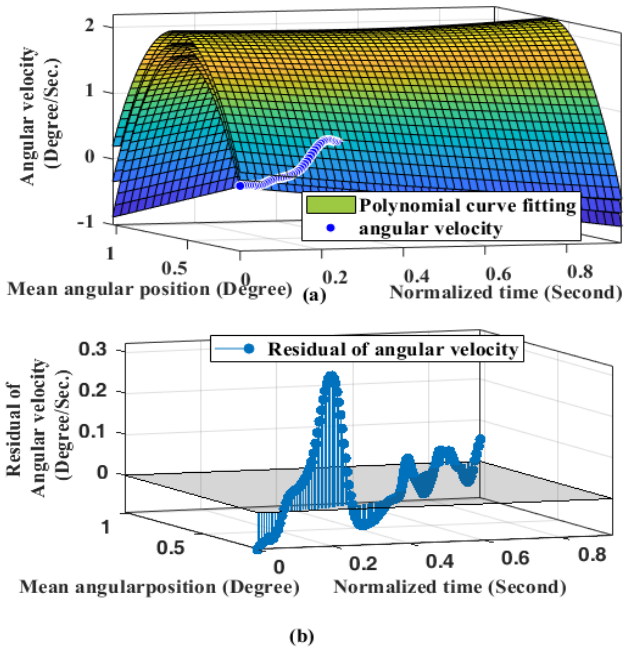

Fig.4: (a) Trajectory of angular position and velocity shown simultaneously with time, and (b) corresponding residual plot.

4. RESULTS AND ANALYSIS

The generation of trajectories are based on the classification of grasping types such as large diameter, small diameter and other types of objects using machine learning algorithms. The predicted model has been generated using appropriate supervised classification algorithms such as quadratic support vector machine (SVM), cubic SVM and SVM with radial basis function (RBF) kernel, random forest classification algorithm (RF) by removing constant, quasi features RF algorithm with only correlated features and recursive feature elimination (RFE) method in RF algorithm.

Table 1. Classification Reports using RFE

Grasping Object Names	Precision	Recall	F1-score	Support
01. Large Diameter	1.00	0.98	0.99	54
02. Small Diameter	0.88	0.86	0.87	50
03. Medium Wrap	0.81	0.87	0.84	54
04. Adducted Thumb	0.86	1.00	0.92	54
05. Light Tool	0.88	0.93	0.90	54
06. Prismatic 4 Finger	0.91	0.94	0.93	53
07. Prismatic 3 Finger	0.96	0.83	0.89	53
08. Prismatic 2 Finger	0.94	0.96	0.95	53
09. Palmar Pinch	0.96	0.88	0.92	50
10. Power Disk	0.81	0.94	0.87	54
11. Power Sphere	0.82	0.83	0.83	54
12. Precision Disk	0.89	0.89	0.89	54
13. Precision Sphere	0.83	0.96	0.89	54
14. Tripod	0.86	0.89	0.87	54
15. Fixed Hook	0.90	0.88	0.89	50
16. Lateral	0.90	0.92	0.91	50
17. Index Finger Extension	0.93	0.94	0.94	54
18. Extension Type	0.82	0.77	0.79	52
19. Distal Type	0.79	0.49	0.60	53
20. Writing Tripod	0.71	0.75	0.73	53
21. Tripod Variation	0.76	0.84	0.80	50
22. Parallel Extension	0.91	1.00	0.95	50
23. Adduction Grip	0.89	0.81	0.85	52
24.Tip Pinch	0.86	0.81	0.83	52
25. Lateral Tripod	0.83	0.81	0.82	54
26. Sphere 4 Finger	0.86	0.75	0.80	51
27. Quadpod	0.87	0.87	0.87	53
28. Sphere 3 Finger	0.89	0.77	0.83	53
29. Stick	0.83	0.94	0.88	51
30. Palmar	1.00	0.90	0.95	50
31. Ring	0.93	0.98	0.95	51
32. Ventral	0.96	0.96	0.96	50
33. Inferior Pincer	1.00	1.00	1.00	50

Using these algorithms, the respective average classification accuracy obtained from them are 32%, 47%, 60%, 70%, 77%, 77% and 88%. Table I shows the classification reports by the generated predictive model using RFE since it has 88% average accuracy. The 'precision' metric is the correctness of the predictive model, where it is the ratio of correctly predicted positive class (true positive or TP) to the total positive predictive classes. Similarly, the 'recall' metric represents the fraction of positive prediction correctly classified. Here, high 'F1-score' metric signifies the harmonic mean between precision and recall value and 'support' metric is the number of actual occurrences. All these metrics computed (Hossin et al., 2015) for Table I, do not change among different models so that it can be used in the evaluation process under various conditions. The metrics considered for classification reports shown in Table 1 are dimensionless as they represent the ratio of successful and unsuccessful grasping of a particular object.

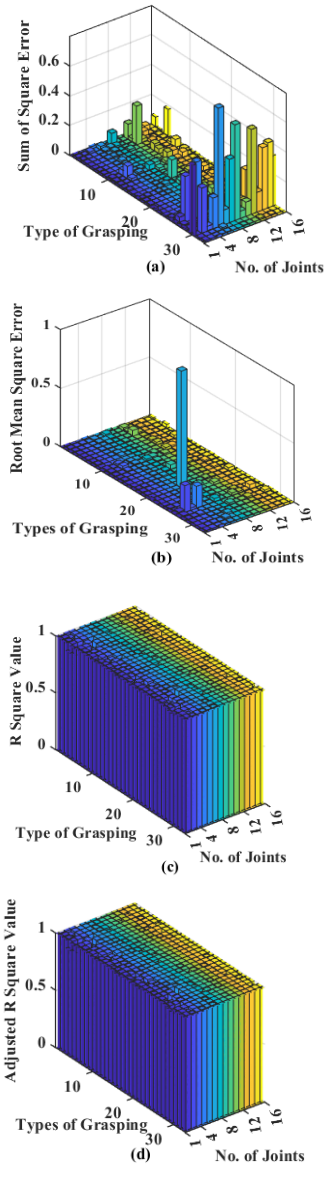

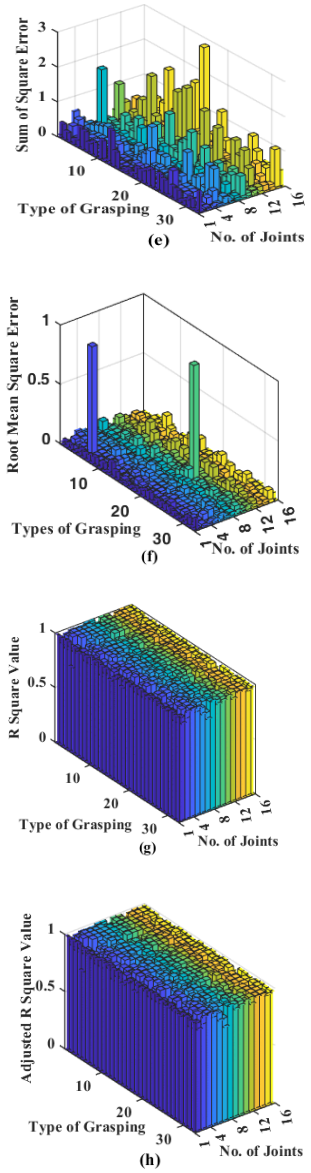

Fig. 5: (a) to (d) depict the SSE, RMSE, R-square and adjusted R-square values respectively for the trajectories of angular postions with time and (e) to (h) illustrate the SSE, RMSE, R-square and adjusted R-square values respectively for the trajectories of velocities with time.

The error metrics such as SSE, RMSE, R-Square and adjusted R-square presented in Fig.5 should maintain their specified thresholds to have proper extension and flexion of each fingers' joints. Fig.5 (a) and (e) illustrate the SSE for angular positions and velocities, which express the deviation between respective generated tractories and the actual angular positions and velocities. These SSE values of angular position trajectories are closer to the one when grasping sphere with 3 fingers, stick, palmar, ring or ventral type objects of all finger joints. Similarly, SSE for velocity trajectories is more than the expected (closer to 0). The average threshold of SSE to grasp all types of objects for angular positions is 0.34 whereas it is 1.0026 for angular velocities. So it is difficult to generate appropriate trajectories of velocities for all types of grasping. As shown in Fig. 5(b)

and 5(f), the RMSE represents the standard deviation of the random data point of angular positions and velocities. The average threshold of RMSE of angular positions and velocities being 0.11 and 0.20 respectively illustrate the small randomness in both angular positions and velocities. From Fig.5(c), (d), (g) and (h) the average threshold for R-square and adjusted R-square of angular positions and velocities are 0.88, 0.85, 0.94 and 0.86 respectively. Hence, the correlation between actual angular positions and velocities with their generated respective trajectories is more considerable for angular positions as compared to angular velocities.

5. CONCLUSION

This study describes a new control system architecture and approach for generating and controlling the stimulation parameters in closed-loop, meant to be applied to the healthy or partially weakened forearm muscles of a paralyzed patient for achieving stable grasping. This is possible to be achieved when the generated stimulation parameters can actuate the muscles in such way that the movement of each finger joints follow the reference trajectories of position and angular velocities, without exceeding their dynamic upper and lower bounds. These reference trajectories of all finger joints to be followed have been successfully generated (and their accuracy suitably characterized through certain metrics) by incorporating and learning from the information of 33 types of objects' stable grasp, after classifying their grasping types. However, very few numbers of generated trajectories (especially for velocities) had difficulties following the upper and lower bounds. So, appropriate measure has to be taken for controlling these trajectories, otherwise uncontrolled stimulation on the muscles may cause early muscle fatigue, restricting the movement of the upper limb. These challenges have to be taken care for ensuring successful and smooth grasping control strategy development. The future work can be that of implementing a data-driven model or a mathematical model of extrinsic or intrinsic muscles for considering the closed-loop strategy control and will be tested for a real object to achieve stable grasping in a clinical environment.

REFERENCES

Bandara, D. S. V., Gopura, R. A. R. C., Kajanthan, G., Brunthavan, M., & Abeynayake, H. I. M. M. (2014, June). An under-actuated mechanism for a robotic finger In *The 4th Annual IEEE International Conference on Cyber Technology in Automation, Control and Intelligent,* pp. 407-412.

Briggs, A.M., Woolf, A.D., Dreinhöfer, K., Homb, N., Hoy, D.G., Kopansky-Giles, D., Åkesson, K. and March, L., (2018). Reducing the global burden of musculoskeletal conditions. *Bulletin of the World Health Organization*, *96*(5), p.366.

Chad, E. B., Ammar , S., Nicholas, V. A., Marcia, A. B., David ,A. F., Dylan ,M. N., Sharma, G., Per, B. S., Bradley, C. G., Mysiw, W.J., Morgan, A.G., Deogaonkar , M., Ali ,R. R., (2016). Restoring cortical control of functional movement in a human with quadriplegia, *Nature*, 533, 247-250.

Chao, E. Y. (1989). Biomechanics of the hand: a basic research study, *World Scientific*.

Djamal, E.C., Suprijanto, S. and Setiadi, S.J., 2016. Classification of EEG-based hand grasping imagination using autoregressive and neural networks. Jurnal Teknologi, 78(6-6).

Feix, T., Pawlik, R., Schmiedmayer, H. B., Romero, J., & Kragic, D. (2009, June). A comprehensive grasp taxonomy. In *Robotics, science and systems: workshop on understanding the human hand for advancing robotic manipulation*(Vol. 2, No. 2.3, pp. 2-3).

Freeman, C.T., 2016. Control system design for electrical stimulation in upper limb rehabilitation. chapter 2. Springer International Publishing, Switzerland:

Friedenberg, D. A., Schwemmer, M. A., Landgraf, A. J., Annetta, N. V., Bockbrader, M. A., Bouton, C. E., & Sharma, G. (2017). Neuroprosthetic-enabled control of graded arm muscle contraction in a paralyzed human. *Scientific reports*, *7*(1), 8386.Djamal,

Li, Z., Guiraud, D., Andreu, D., Gelis, A., Fattal, C., & Hayashibe, M. (2018). Real-Time closed-loop functional electrical stimulation control of muscle activation with evoked electromyography feedback for spinal cord injured patients. *International journal of neural systems*, *28*(06), 1750063.

Mattar, E. A., Al-Junaid, H. J., & Al-Seddiqi, H. H. (2017). Biomimetic Based EEG Learning for Robotics Complex Grasping and Dexterous Manipulation. In *Biomimetic Prosthetics*. IntechOpen.

Paul, L. C., Suman, A. A., & Sultan, N. (2013). Methodological analysis of principal component analysis (PCA) method. *International Journal of Computational Engineering & Management*, *16*(2), 32-38.

Roy, R., Sikdar, D., Mahadevappa, M., & Kumar, C. S. (2018). A fingertip force prediction model for grasp patterns characterised from the chaotic behaviour of EEG. *Medical & biological engineering & computing*, *56*(11), 2095-2107..

Santello, M., Flanders, M., & Soechting, J. F. (2002). Patterns of hand motion during grasping and the influence of sensory guidance. *Journal of Neuroscience*, *22*(4), 1426-1435.

Sburlea, A. I., & Müller-Putz, G. R. (2018). Exploring representations of human grasping in neural, muscle and kinematic signals. *Scientific reports*, 8(1), 16669.

Westerveld, A. J., Kuck, A., Schouten, A. C., Veltink, P. H., & van der Kooij, H. (2012, August). Grasp and release with surface functional electrical stimulation using a Model Predictive Control approach. In *2012 Annual International Conference of the IEEE Engineering in Medicine and Biology Society* (pp. 333-336). IEEE.

Yong, X., & Menon, C. (2015). EEG classification of different imaginary movements within the same limb. *PloS one*, *10*(4), e0121896.

Hossin, M., & Sulaiman, M. N. (2015). A review on evaluation metrics for data classification evaluations. International Journal of Data Mining & Knowledge Management Process, 5(2), 1.